UC Berkeley

UC Berkeley Previously Published Works

Title

Data on biomechanics and elemental maps of dental implant-bone complexes in rats

Permalink

https://escholarship.org/uc/item/6jc4c5n3

Authors

Wang, B
Kim, K
Srirangapatanam, S
et al.

Publication Date

2020-08-01

DOI

10.1016/j.dib.2020.105969

Peer reviewed

Data Article

Data on biomechanics and elemental maps of dental implant-bone complexes in rats

B. Wang [a],[*], K. Kim [a],[*], S. Srirangapatanam [b], P. Ustriyana [a],
S.E. Wheelis [c], S.C. Fakra [d], M. Kang [a], D.C. Rodrigues [c], S.P. Ho [a],[b],[*]

[a] Department of Preventive and Restorative Dental Sciences, School of Dentistry, UCSF, San Francisco, CA 94143, USA
[b] Department of Urology, School of Medicine, UCSF, San Francisco, CA 94143, USA
[c] Department of Bioengineering, University of Texas at Dallas, Dallas, TX 75080, USA
[d] Advanced Light Source, Lawrence Berkeley National Laboratory, Berkeley, CA 94720, USA

ARTICLE INFO

ABSTRACT

Implant-bone biomechanics and mechanoadaptation of peri–implant tissue in space (around and along the length of an implant) and time (3-, 11-, and 24-day following implantation) are important for functional osseointegration of dental implants. Spatiotemporal shifts in biomechanics of implant-bone complex in rat maxillae were correlated with maximum (tensile) and minimum (compressive) principal strain profiles in peri–implant tissue using a hybrid model; biomechanics *in situ* paired with digital volume correlation. Spatiotemporal changes in elemental counts and their association with mineral density of the peri–implant tissue were mapped using electron dispersive X-ray and X-ray fluorescence microprobe techniques. Data provided within are related to biomechanical testing of an implant-bone complex *in situ*. Data also highlight the power of correlating elemental colocalization with tension and compression regions of the peri–implant tissues to explain spatiotemporal mechanoadaptation of implant-bone complexes. Further interpretation

Specifications table

Subject	"Mechanics of Materials" or "Biomaterials" or "Dentistry, Oral Surgery and Medicine"
Specific subject area	Biomechanics
Type of data	Figure
	Movie
	Table
How data were acquired	Biomechanics data were acquired *in situ* using tension/compression stage (MT10352, 500 N Nano Tomography, Deben UK Limited) coupled to a micro X-ray computed tomography (micro XCT, MicroXCT-200, Carl Zeiss X-ray Microscopy). X-ray tomograms were analyzed using image analysis software (AVIZO, FEI Visualization Sciences Group). Displacement of the implant in association with the peri–implant tissue was registered as a load-displacement curve. Tomograms of IBC at no load and under loaded conditions were reconstructed into three-dimensional (3D) volumes respectively. These 3D volumes at no load and under load were correlated digitally to generate tension and compression strain profiles using a software written in $C++$ language. Elemental maps of carbon (C), sulfur (S), calcium (Ca), and phosphorus (P) were obtained using electron dispersive X-ray spectroscopic technique (EDX, Quantax EDS, Bruker Nano Inc.). Peri-implant tissue structure was imaged at a higher resolution using a scanning electron microscope (SEM, Zeiss SIGMA 500-VP Field Emission Electron Microscope). Elemental maps including zinc (Zn), Ca, and P were generated using X-ray fluorescence (XRF) microprobe, beamline 10.3.2 of Advanced Light Source (ALS) at Lawrence Berkeley National Laboratory (LBL).
Data format	Raw
	Analyzed
Parameters for data collection (400 characters max)	Biomechanics data using different loads were collected on the implant-bone complex (IBC) within rat hemimaxillae (cubical shape of $\sim 5 \times 5 \times 4\,mm^3$). Biomechanical testing of IBCs following 3-, 11-, and 24-day of implantation was performed using a fixed loading rate of 0.2 mm/min. A single stepwise compression test was performed on IBC at 3-day time point. The biomechanics of the 3-day IBC was tested to four peak loads (4 N, 8 N, 12 N, failure load) but at the same loading rate of 0.2 mm/min.
Description of data collection (600 characters max)	Both fixed and stepwise compression tests on IBC were conducted on a compression stage. Mechanical testing was paired with imaging using a micro XCT. Following compression test, tomograms were analyzed using AVIZO software to obtain contact area of peri–implant tissue with implant. Additionally, bone mineral density, and bone volume fraction also were evaluated from X-ray tomograms. To map strain localization within peri–implant tissue, tomograms of IBC at no load and under loaded conditions were reconstructed into three-dimensional (3D) volumes. These 3D volumes at no load and under load were correlated digitally using a software written in $C++$ language to generate negative (compressive) and positive (tensile) strain profiles. Specimens were subsequently embedded in epoxy resin and were polished to mirror finish to generate elemental maps using EDX and XRF microprobe techniques.
Data source location	Department of Preventive and Restorative Dental Sciences, School of Dentistry, University of California, San Francisco, CA, USA.
Data accessibility	The data are available with the article.
Related research article	Wang, B., Kim, K., Srirangapatanam, S., Ustriyana, P., Wheelis, S. E., Fakra, S., Kang, M., Rodrigues, D. C., Ho, S. P., Mechanoadaptive strain and functional osseointegration of dental implants in rats, Bone 137 (2020). https://doi.org/10.1016/j.bone.2020.115375.

Value of the data

- These experimental conditions would enable researchers to perform: **1) Biomechanical testing of intact specimens:** The described biomechanical testing *in situ* will provide an accurate estimate of differences and changes in joint biomechanics and implant-tissue complexes within a group and across groups. Often, biomechanical testing is performed on specimens reduced to size and shape to fit experimental conditions and specimen-stage of a mechanical testing apparatus. It minimizes experimental variability and artifacts as specimens are kept intact and biomechanical testing is performed under wet conditions, a physiologically relevant condition; **2) Correlation of implant-bone complex (IBC) volume at no load with IBC volume at loaded conditions to evaluate peri–implant tissue deformation:** Correlating spatial coordinates of voxels under conditions of no load and under load enables generating deformation maps with no material property assumptions; **3) Correlation between data sets including mechanical strain, elemental composition and mineral density:** Spatial correlation between mechanical strain, mineral density, and elemental composition data sets will provide information on the changes in material properties of strained IBCs. This testing method facilitates mapping of mechanoadaptation of IBC in space and over time (biomechanical testing *in situ*) with high-resolution imaging techniques (micro XCT, electron microscopy, and energy dispersive X-ray spectroscopy and XRF microprobe).
- These data are of particular interest to researchers within the following fields of research: dental and orthopedic biomaterials and implants, biomechanics of tissues and joints, correlative spectroscopy and microscopy, and biomaterials as related to tissue regeneration and engineering.
- These data, along with the experimental parameters, serve as an overview and a reference for biomechanics of an IBC. The data demonstrate biomechanical capacity of an IBC to sustain function, which is parameterized as magnitude, frequency, and duration of load. Development of experiments performed *in situ* on a rodent model can include fatigue-related experiments on IBC, and mapping contact mechanics and related tissue deformation in maxillary and mandibular interdigitating bodies.
- These data, especially strain localization, can be used as a reference to guide implant design for accelerating osseointegration following implantation.

1. Data description

Figs. 1a and 1b show color maps representing surface distance between the dental implant and the inorganic peri–implant tissue (bone) at different time points: 3-, 11-, and 24-day after implantation. Fig. 1c provides average distance and contact conditions between the surface of implant and bone at different time points.

Movie 1 illustrates a reconstructed virtual 3D volume of an IBC at 11-day time point. The red color represents the organic portion of the peri–implant tissue around the implant, while the gray shows the inorganic portion of the peri–implant tissue.

Table 1 consists of dataset for load *vs.* displacement relationship from biomechanics experiments *in situ*. There are four different worksheets, including load *vs.* displacement data for each fixed compression test at 3-, 11-, and 24-day time points, and for stepwise compression test at 3-day time point.

Fig. 2A shows the setup of the loading stage for a stepwise compression test and micro X-ray computed tomography (micro XCT) imaging, with the corresponding load-displacement curve and reconstructed virtual section at 0 N. Stepwise strain responses in peri–implant tissue at 3-day time point are shown in Fig. 2B.

Movie 2 shows the movement of a dental implant relative to bone at different loads. Tomograms of the same region but at different loads were superimposed to illustrate the movement of the implant relative to bone during stepwise compression test.
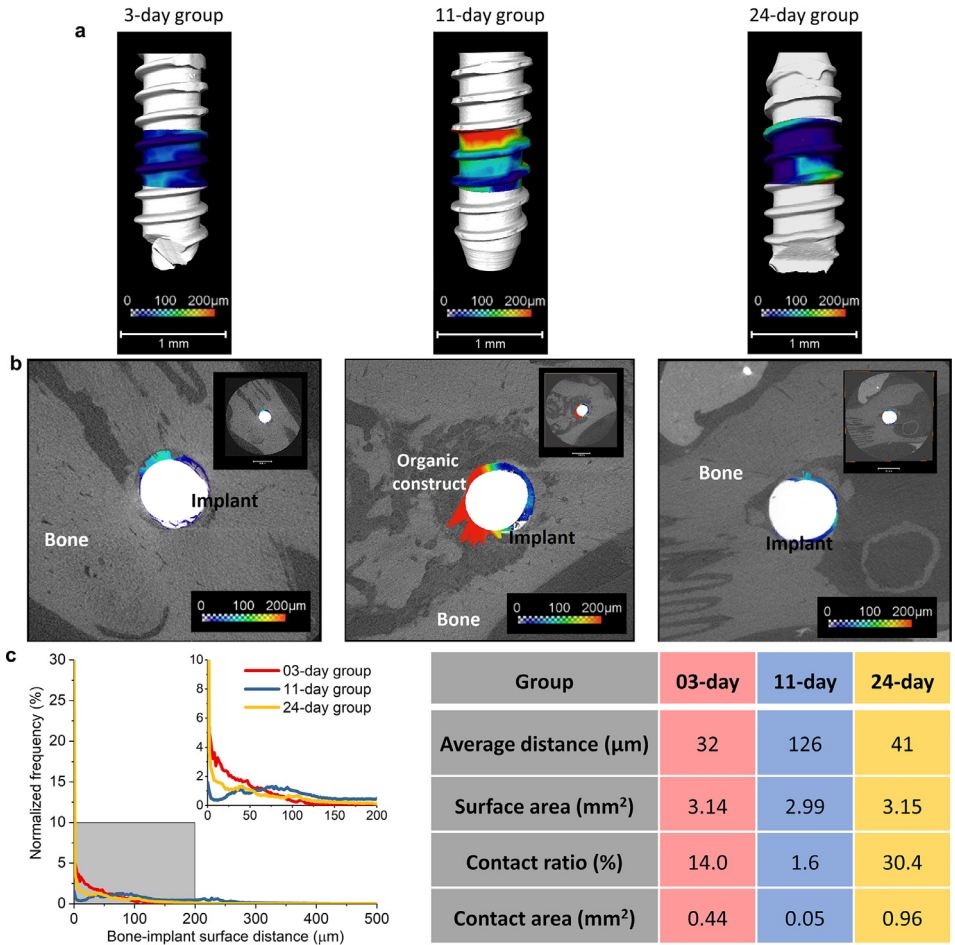
Fig. 1. Surface distance and contact between mineralized peri–implant tissue (bone) and implant surface at different time points after implantation (left: 3-day, middle: 11-day, right: 24-day); (a) color maps of surface distance projected on three-dimensional (3D) volumes of the IBCs; (b) 2D virtual transverse sections of corresponding IBCs with surface distances; (c) graph of normalized frequency of surface distances and table with implant-bone contact values at different time points are shown.

Table 2 contains 2 worksheets of maximum and minimum principal strains and frequency of their occurrence resulting from stepwise loading to peak loads of 4 N, 8 N, 12 N, and 18 N of a 3-day IBC.

Movie 3 demonstrates the progressive change in maximum principal strain resulting from stepwise loading to peak loads of 4 N, 8 N, 12 N, and 18 N of a 3-day IBC.

Movie 4 demonstrates the progressive change in minimum principal strain maps of a 3-day time point IBC resulting from stepwise loading to peak loads of 4 N, 8 N, 12 N, and 18 N.

Fig. 3A illustrates structure of an 11-day IBC using a scanning electron microscope (SEM). Fig. 3B shows elemental maps of regions indicated in orange and magenta boxes in the lower magnification SEM image of a 11-day IBC. Elemental maps were obtained from electron dispersive X-ray spectroscopy (EDS). Spectra and quantitative maps of areas 1–3 also are shown in Fig. 3B. The corresponding elemental (Ca, P, Zn) maps obtained from X-ray fluorescence (XRF) microprobe were published by Wang et al. [1].

Table 3 contains raw dataset from energy dispersive X-ray analysis (EDX). Data for each area in Fig. 3B also are included in seperate worksheets in Table 3.
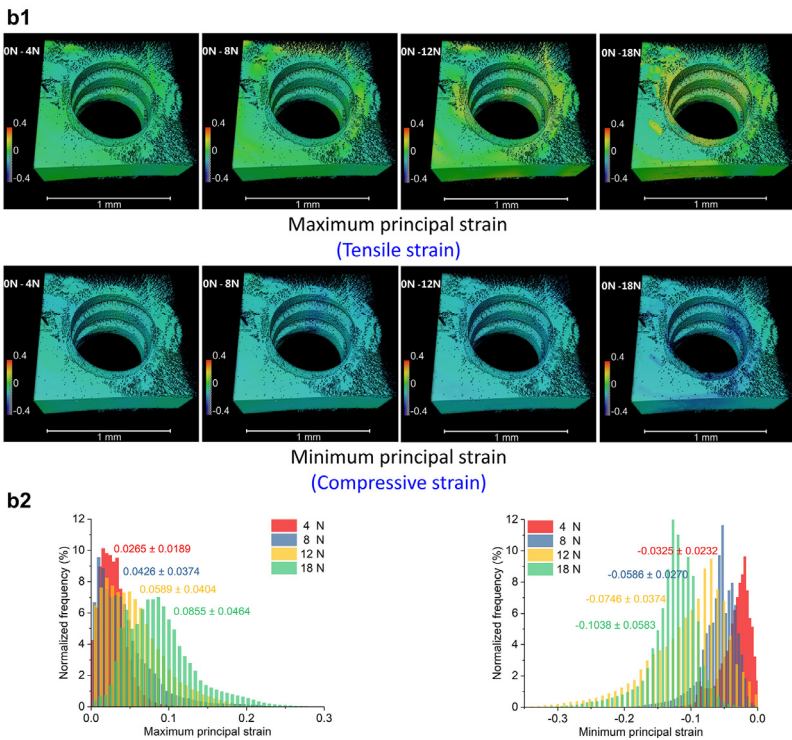
A. Stepwise loading of the implant-bone complex
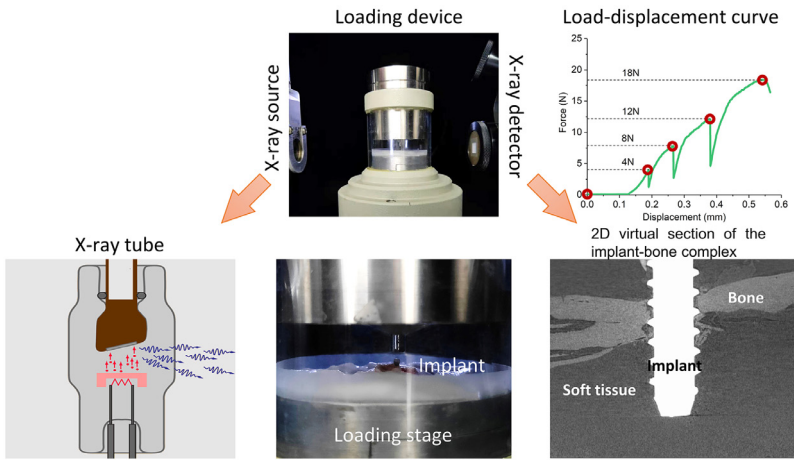
Fig. 2. (A) A schematic of stepwise compression test and X-ray imaging of IBC at 3-day time point following implantation; (B) tensile and compressive strain maps in peri–implant tissue under stepwise compression at different loading stages (4 N, 8 N, 12 N, and 18 N) (b1); and the normalized frequency of maximum and minimum principal strains in the peri–implant tissue at different loads (b2) are shown in this figure.
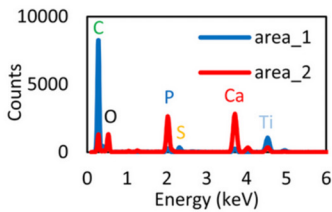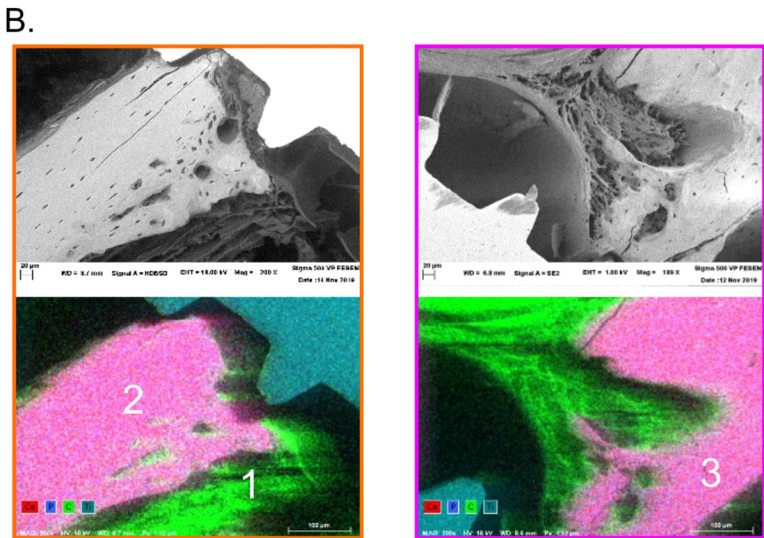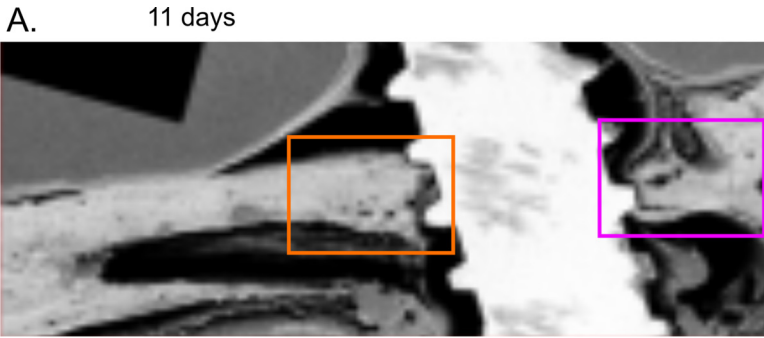
Fig. 3. Structure and elemental distributions of an 11-day IBC; (A) SEM micrograph of an IBC at 11-day time point, scale bar: 1 mm; (B) micrographs at 200× magnification of peri–implant tissue and dental implant at 11-day time point; spatial quantitative maps of elements, such as C, Ca, P, and Ti, and X-ray spectra of the IBC by EDX and relative values are shown in this figure.

2. Experimental design, materials, and methods

### 2.1. Mechanical compression test of the IBC in situ

A tension/compression stage (MT10352, 500 N Nano Tomography, Deben UK Limited) coupled to a micro XCT system (MicroXCT-200, Carl Zeiss X-ray Microscopy, Pleasanton, CA, USA) was
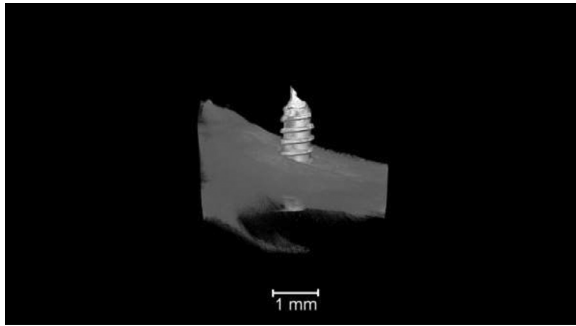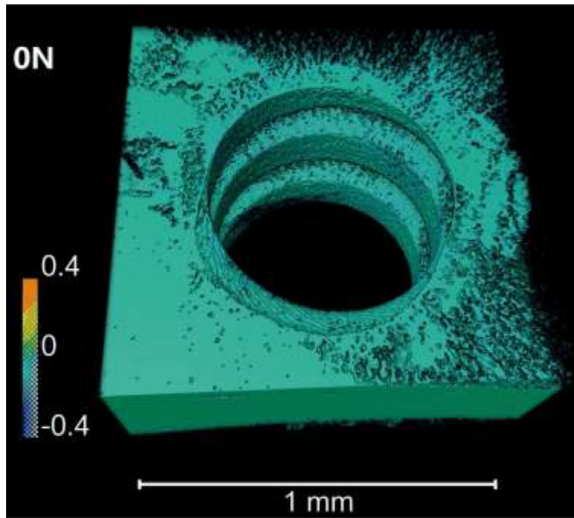
Movie 1. Movie of 3D volume of IBC with organic and inorganic peri–implant tissues highlighted in red and gray, respectively.
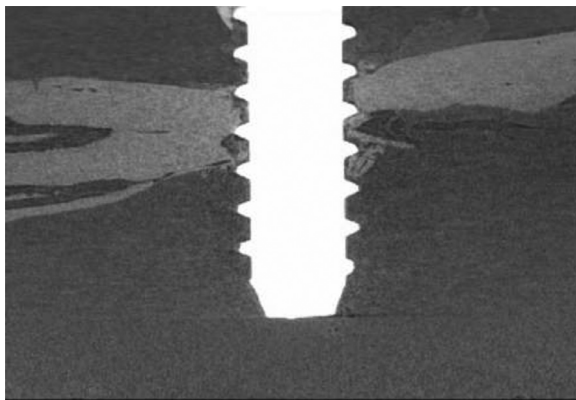
Movie 2. Movement of dental implant relative to bone under stepwise compressive loads of 4 N, 8 N, 12 N, and 18 N.
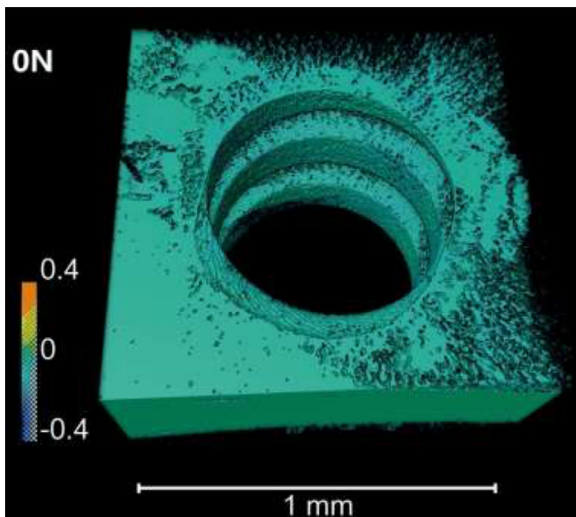
Movie 3. Progressive tensile strain map in response to stepwise compressive loads on a 3-day IBC.

Movie 4. Progressive compressive strain map in response to stepwise compressive loads on a 3-day IBC.

used for compression tests *in situ*. The IBCs were sectioned into cubes of $\sim 5 \times 5 \times 4\,mm^3$ from rat hemimaxillae. To avoid eccentric loads, all specimens were loaded along the longitudinal axis of the implant. Specimens were immobilized on the loading stage using polymethylmethacrylate (PMMA). The IBC was uniformly loaded parallel to the loading anvil by mounting a dental composite on top of the implant.

The specimens from three time points (3-, 11-, 24-day) were loaded at a rate of 0.2 mm/min until failure of the IBC was registered as a sudden drop in the reactionary force-displacement curve. The stiffness of the IBC was calculated as the slope of the reactionary force-displacement curve. Micro XCT images (spatial resolution: ~ 4.16 mm/voxel, X-ray source energy: 90 kV, magnification: 4X) were collected at no load and at peak load to failure.

A stepwise compression test was conducted on a 3-day IBC using the same experimental devices and setup. The 3-day IBC was serially loaded to 4 N, 8 N, 12 N, and subsequently to failure at a loading rate of 0.2 mm/min. A 5-min wait period was set to equilibrate the IBC prior to imaging using a micro XCT.

Upon imaging, tomograms were reconstructed to obtain a) contact area of the peri–implant tissue with the implant, b) bone mineral density, and c) bone-volume fraction using surface distance, watershed and image segmentation algorithms in AVIZO software (FEI Visualization Sciences Group).

2.2. Spatiotemporal strain maps of the IBC

Strain localization in the peri–implant tissues at 3-, 11- and 24-day were mapped using digital volume correlation (DVC) algorithm respectively. DVC was performed by correlating the voxels of the IBC at no load to loaded conditions. A domain with a size of $\sim 250 \times 250 \times 140$ voxel^3 (physical size: $1.04 \times 1.04 \times 0.58\,mm^3$) surrounding the dental implant was selected as the region of interest. Calculation points were evenly distributed within peri–implant tissue at a grid step of 2 voxels. A sub-volume size of $41 \times 41 \times 41$ voxel^3 (physical size: $0.17 \times 0.17 \times 0.17\,mm^3$) was used at each calculation point. Maximum/minimum principal strains were defined as the extreme normal strains at a point occurring in the plane where shear strains are zero (theoretically). All DVC analyses were performed using a software written in *C++* language as previously described [2].

2.3. Spatiotemporal elemental maps of the IBC

Unloaded specimens were imaged at 4X magnification ($\sim$5 μm/pixel; 50 kVp) using micro XCT. The specimens were prepared for XRF microprobe as follows: 1) epoxy resin embedding; 2) hemi-sectioned using a slow speed saw; 3) surface-polished to a mirror finish using a series of diamond suspension slurries (6, 3, 2, 1, and 0.5 μm). Elemental maps including calcium (Ca), phosphorus (P), and zinc (Zn) from sectioned specimens at 3- and 11-day time points were collected using the XRF microprobe (incident photon energy: 10 keV; spot size: $\sim$5 $\times$ 5 μm) at beamline 10.3.2 of the Advanced Light Source (ALS) at Lawrence Berkeley National Laboratory (LBNL), Berkeley, CA, USA [3].

Relative grey scale differences in arbitrary units (a.u.) were used to map relative differences in mineral densities of peri–implant tissues within and across groups. Multiple micro XCT slices of IBC within each group were selected and averaged to account for the XRF microprobe penetration depth, and for accurate spatial correlation of mineral density and elemental maps of the same specimen. The averaged micro XCT tomograms were adjusted in size to spatially register with the XRF microprobe elemental maps using AVIZO. Ca, P, and Zn maps were segmented into Ca-, P-, and Zn-enriched regions based on a threshold of mean plus standard deviation. MD analysis within the region was performed after extracting MD maps corresponding to Ca-, P-, and Zn-enriched spatial coordinates. This spatial association was performed to correlate elemental counts to MD.

Specimens also were imaged for micro-struccture visualization using SEM (Zeiss SIGMA 500-VP Field Emission Electron Microscope; energy: 1 keV; high pressure chamber) followed by elemental characterization using energy dispersive X-ray spectroscopy (Quantax EDS, Bruker Nano Inc.) to collect spectra of C, Ca, P, and Ti at each pixel at an electron energy of 18 keV in a variable pressure mode.

Declaration of Competing Interest

The authors declare that they have no known competing financial interests in the publication of this article. The authors submitted this article along with an invited research article in Bone, special issue in Musculoskeletal Imaging.

Acknowledgments

Supplementary materials

Supplementary material associated with this article can be found, in the online version, at doi:10.1016/j.dib.2020.105969.

References

[1] B. Wang, K. Kim, S. Srirangapatanam, P. Ustriyana, S.E. Wheelis, S. Fakra, M. Kang, D.C. Rodrigues, S.P. Ho, Mechanoad-aptive strain and functional osseointegration of dental implants in rats, Bone 137 (2020), doi:10.1016/j.bone.2020.115375.
[2] B. Wang, B. Pan, Self-adaptive digital volume correlation for unknown deformation fields, Exp. Mech. 59 (2019) 149–162, doi:10.1007/s11340-018-00455-2.
[3] M.A. Marcus, A.A. MacDowell, R. Celestre, A. Manceau, T. Miller, H.A. Padmore, R.E. Sublett, Beamline 10.3.2 at ALS: a hard X-ray microprobe for environmental and materials sciences, J. Synchrotron Radiation 11 (2004) 239–247, doi:10.1107/S0909049504005837.